arXiv:1609.01173v1 [cond-mat.stat-mech] 5 Sep 2016

Reaction Spreading in Systems With Anomalous Diffusion

F. Cecconi
CNR - Istituto dei Sistemi Complessi
Via dei Taurini 19, I-00185 Rome, Italy
D. Vergni
CNR - Istituto Applicazioni del Calcolo
Via dei Taurini 19, I-00185 Rome, Italy
A. Vulpiani
Università di Roma "Sapienza"
Piazzale A. Moro 5, I-00185 Rome, Italy.

September 6, 2016

Abstract

We briefly review some aspects of the anomalous diffusion, and its relevance in reactive systems. In particular we consider *strong anomalous* diffusion characterized by the moment behaviour $\langle x(t)^q \rangle \sim t^{q\nu(q)}$, where $\nu(q)$ is a non constant function, and we discuss its consequences. Even in the apparently simple case $\nu(2) = 1/2$, strong anomalous diffusion may correspond to non trivial features, such as non Gaussian probability distribution and peculiar scaling of large order moments.

When a reactive term is added to a normal diffusion process, one has a propagating front with a constant velocity. The presence of anomalous diffusion by itself does not guarantee a changing in the front propagation scenario; a key factor to select linear in time or faster front propagation has been identified in the shape of the probability distribution tail in absence of reaction. In addition, we discuss the reaction spreading on graphs, underlying the major role of the connectivity properties of these structures, characterized by the *connectivity dimension*.

1 Introduction

Transport processes and, in particular, diffusion play a very important impact in science and technology [49], among the many examples about their relevance we can mention their role in Geophysics, e.g. pollutant spreading in atmosphere [46] or oceans [53], in Biology and Chemistry as a framework to the interpretation of pattern formation and growth mechanisms [42], and finally in Mathematics for their connection with stochastic processes [51], including the historical importance of the Brownian motion for the understanding of the physical reality of atoms [31].

From a mathematical perspective, a transport process can be seen as a class of deterministic or stochastic rule for the time evolution $\mathbf{x}(0) \to \mathbf{x}(t) = \mathcal{S}^t\mathbf{x}(0)$, where $\mathbf{x}$ belongs to an unbounded domain and $|\mathbf{x}|$ typically increases with time. Likely, the paradigmatic example of a transport process is given by a stochastic differential equation ruling the time evolution of a fluid particle:

$$\frac{d\mathbf{x}}{dt} = \mathbf{u}(\mathbf{x}, t) + \sqrt{2D}\boldsymbol{\eta}(t) \,, \tag{1.1}$$

where $\boldsymbol{\eta}(t)$ is a white noise, D is the particle self-diffusivity and $\mathbf{u}(\mathbf{x}, t)$ is a given velocity field driving the fluid, typically incompressible: $\nabla \cdot \mathbf{u} = 0$.

We can associate to the above-mentioned dynamics an equation for the time evolution of the probability density function (PDF) $P(\mathbf{x}, t)$. In this case one obtains the advection diffusion equation (also known as Fokker-Planck equation)

$$\frac{\partial P}{\partial t} + (\mathbf{u} \cdot \nabla)P = D\Delta P \,. \tag{1.2}$$

Usually the explicit solution to Eq. (1.2) cannot be worked out, however, for many purposes and applications, the knowledge of the asymptotic behaviour of the solution is sufficient to understand some basic properties of the transport process. At large scale and asymptotically in time, the so called *normal diffusion* is typically expected [34], i.e. a Fick's law give an accurate approximation for the evolution of $\tilde{P}$, that is the spatial coarse-graining of P,

$$\frac{\partial \tilde{P}}{\partial t} = \sum_{i,j} D^e_{ij} \frac{\partial^2 \tilde{P}}{\partial x_i \partial x_j} \tag{1.3}$$

where

$$\langle x_i(t) x_j(t) \rangle \simeq 2D^e_{ij} t \,.$$

and D^e_{ij} is the effective (eddy) diffusion tensor [17], [34] depending, often in a not trivial way, on both D and $\mathbf{u}$. We considered just for simplicity the case without average drift, $\langle \mathbf{x} \rangle = 0$. Eq. (1.3) implies a Gaussian behaviour for $\tilde{P}$:

$$\tilde{P}(\mathbf{x}, t) \sim \exp\left\{ -\frac{1}{4t} \sum_{i,j} x_i \, [D^e]^{-1}_{ij} \, x_j \right\} . \tag{1.4}$$

This common scenario is the simplest generalization of the pure-diffusion case, where $\mathbf{u} = 0$ and $D^e_{ij} = D\delta_{ij}$, and the presence of the velocity field $\mathbf{u}$ has only a quantitative effect for the values of the D^e_{ij}, but the Gaussian behaviour is still valid.

Two questions naturally arise: a) is the normal diffusion a meaningful approximation? b) how could the asymptotic behaviour of a transport process result in a violation of the Fick's law (1.3)?

We will discuss some features of the so called anomalous diffusion where we have a failure of the previous scenario: $\langle x^2(t) \rangle \sim t^{2\nu}$ with $\nu \neq 1/2$ and a $P(\mathbf{x}, t)$ that is not Gaussian. We will see that *anomalous diffusion* is a consequence of the violation of the hypothesis of the central limit theorem (CLT). It is important to remark that there are cases in which anomalous behaviour can be rigorously proved (as in the case of Lévy-stable distribution). Moreover we also consider the case of *strong* anomalous diffusion, when $\langle x(t)^q \rangle \sim t^{q\nu(q)}$ and $\nu(q)$ is a non constant function. In addition, we will also discuss the diffusion on discrete structure "*spatially*" non homogeneous like graphs. In such systems, e.g. in the case of a "fractal" structure of the graphs, one can have anomalous diffusion.

In chemistry, biology and physics it is rather common that, in specific medium or environments, the transport phenomena are accompanied to, or even driven by, transformations or competitions among chemical or biological species [43]. Thus Eq.(1.2) needs to be modified by introducing some extra term describing such reactions. In this context, we can mention the simplest reaction-diffusion equation introduced by Fisher [20] and Kolmogorov, Petrovkii and Piskunov [32]: a one-dimensional system with normal diffusion and a reactive term:

$$\frac{\partial \theta}{\partial t} = D \frac{\partial^2}{\partial x^2} \theta + \frac{1}{\tau} f(\theta) \, , \tag{1.5}$$

where the quantity $\theta(x, t)$ represents the concentrations of a chemical or biological species. The term $f(\theta) = \theta(1 - \theta)$ describes an autocatalytic reaction which allows for the transformation from the unstable state ($\theta = 0$) to the stable state ($\theta = 1$). In an unbounded domain,

Eq. (1.5) is known to admit travelling wave solutions moving at a constant speed $v_f = 2\sqrt{Df'(0)/\tau}$ [20], [32].

One can wonder how the propagation behaviour of the system can change when considering more general transport processes with a non-normal diffusive behaviour, e.g., when either the Laplacian in Eq. (1.5) is replaced by another linear operator or the dynamics spans the *"spatially"* discrete structure of a graph. We will see that the presence of anomalous diffusion is not sufficient to induce a nonlinear front propagation in the presence of a reaction. Such a result can be understood, at least in some cases, with a linear analysis starting from the shape of the $P(x,t)$ tail in the reaction free system.

The paper is organized as follows: in Sect. 2 we briefly survey possible mechanisms that, violating the CLT hypothesis, lead to anomalous transport. In particular, we focus on processes where the anomalous behaviour is induced by: the statistical properties of the advecting fields, the stochastic nature of the dynamics, or by restraining the random walks on specific graph-like structures. In Sect. 3, we discuss the effect of the anomalous diffusive motion of reactants on the propagation front in reaction diffusion systems. In Sect. 4, we consider some cases where the anomalous transport is due to the graph-like geometry of the domain where the reaction diffusion takes place. Sect. 5 contains some conclusions.

2 Mechanisms for anomalous diffusion

This section is devoted to the discussion of diffusion processes described by the superposition of many elementary displacements

$$\mathbf{x}(t+h) = \mathbf{x}(t) + h\mathbf{v}(\mathbf{x}(t), t). \tag{2.1}$$

where h is a constant of the dimension of time, the term $\mathbf{v}(\mathbf{x}(t), t)$, defining the character of the displacement, embodies both deterministic and stochastic elements, as for the case of Brownian particles advected by a velocity field. Eq. (2.1) includes also the case of the motion over complex discrete structures when the displacements are identified with the links of a graph.

We shall see through the following examples, how the statistical properties of the dynamics generated by the rule (2.1) depends on the correlation of the elementary displacements [25]. When such correlations allow the central limit theorem to be applicable, the dynamics obeys the normal diffusion, when not, anomalous behaviours could take place. However as reported in [30], there exist cases in which

linear mean square displacement does not necessarily imply a Gaussian behaviour of the probability distribution. In particular, we consider hereafter cases in which this correlation is already intrinsic in $\mathbf{v}(\mathbf{x}(t), t)$ and cases in which it is imposed by the geometric structure of the graph which constitutes the support to the displacements.

In the limit $h \to 0$, the elementary displacements become infinitesimal, thus, the evolution (2.1) turns out to be continuous in time and can be generally written as the stochastic differential equation (1.1).

Equivalently, we can consider the evolution of the PDF of $\mathbf{x}$

$$\partial_t P = \hat{L} P \,, \tag{2.2}$$

where the linear operator $\hat{L}$ accounts for the global transport properties of the system, i.e., the macroscopic operator describing the composition of the microscopic term $\mathbf{v}(\mathbf{x}(t), t)$.

In Section 2.1, we firstly investigate the conditions under which the transport process (2.1) exhibits a normal diffusion behaviour for large times, then we discuss different models that can be used to describe transport processes focusing on examples able to show anomalous diffusion. In particular we start from advection-diffusion models, where $\hat{L} = -\mathbf{u} \cdot \nabla + D\Delta$, passing through transport in 2D Hamiltonian system, and finally ending to the mesoscale effective diffusion models suitable to study transport properties in turbulent flow and heterogeneous media [44], where $\hat{L} = \frac{1}{r^{d-1}} \frac{\partial}{\partial r} \left(k(r) r^{d-1} \frac{\partial}{\partial r} \right)$. In Section 2.2 stochastic processes, and in particular continuous time random walk are investigated as an example of transport dynamics showing strong anomalous diffusion characterized by the behaviour $\langle |x(t)|^q \rangle \sim t^{q\nu(q)}$ of its moments, where $\nu(q)$ is a non constant function. Then, in Section 2.3, diffusion processes in discrete systems with a non homogeneous spatial structure are taken into account.

2.1 Anomalous diffusion in presence of velocity fields

Here we consider the evolution of a test Brownian particle advected by the incompressible velocity field $\mathbf{u}$, described by the stochastic differential equation (1.1). Let us recall the Taylor-Kubo relation [34] between diffusion coefficient and velocity-velocity correlation function: a direct integration of equation (1.1) provides easily the mean square

displacement:

$$\langle [x_i(t) - x_i(0)]^2 \rangle = \int_0^t dt_1 \int_0^t dt_2 \langle v_i(\mathbf{x}(t_1))\, v_i(\mathbf{x}(t_2)) \rangle \simeq 2\, t \int_0^t d\tau\, C_{ii}(\tau)\,, \tag{2.3}$$

where

$$C_{ij}(\tau) = \langle\, v_i(\mathbf{x}(\tau))\, v_j(\mathbf{x}(0))\, \rangle \tag{2.4}$$

is the correlation function of the Lagrangian velocity in Eq.(1.1)) and $\mathbf{v} = \dot{\mathbf{x}}$ (see Eq. (2.1)). If the hypothesis of the central limit theorem are satisfied:

a) finite variance of the velocity, i.e., $\langle |\mathbf{v}|^2 \rangle < \infty$,

b) fast enough decay of $R_{ii}(\tau) = C_{ii}(\tau)/\langle v_i^2 \rangle$, i.e, $0 < \int_0^t \mathrm{d}\tau\ \mathrm{R_{ii}}(\tau) < \infty$,

a normal diffusion takes place and we can define an eddy diffusivity as

$$D^e_{ii} = \lim_{t\to\infty} \frac{1}{2t} \langle |x_i(t) - x_i(0)|^2 \rangle = \langle v_i^2 \rangle \int_0^\infty \mathrm{d}\tau\ R_{ii}(\tau)\,. \tag{2.5}$$

The previous considerations are still valid for test particle evolving according to a discrete time map

$$\mathbf{x}(n+1) = \mathbf{f}(\mathbf{x}(n))\,;$$

with the obvious changes

$$\mathbf{v} \Rightarrow \mathbf{f}(\mathbf{x}) - \mathbf{x} \qquad \text{and} \qquad \int_0^t \mathrm{d}\tau C_{ii}(\tau) \Rightarrow \frac{C_{ii}(0)}{2} + \sum_{k=1}^{n} C_{ii}(k)\ . \tag{2.6}$$

On the contrary, if at least one of the hypothesis of the CLT fails, the transport process could not be a normal diffusion. Therefore a finite D^e_{ii} cannot be defined: formally $D^e_{ii} = \infty$ (superdiffusion) or $D^e_{ii} = 0$ (subdiffusion). The reader should note that super diffusion appears when either the integral $\int_0^t d\tau\ C_{ii}(\tau)$ in Eq. (2.3) or the sum $\sum_{k=1}^n C_{ii}(k)$ in Eq. (2.6), diverges.

A very important result about anomalous diffusion in incompressible velocity fields was obtained in [5] and [6] and can be summarized as follows. If the molecular diffusivity D is non zero, and the infrared contribution from the Fourier components $\hat{\mathbf{u}}(\mathbf{k})$ of the velocity field are weak enough, namely

$$\int d\mathbf{k}\ \frac{\langle |\hat{\mathbf{u}}(\mathbf{k})|^2 \rangle}{k^2} < \infty\,, \tag{2.7}$$

then the advected fluid particles undergo normal diffusion, i.e., the effective diffusion coefficients D^e_{ii}'s in (2.5) are finite. The symbol $\langle \cdot \rangle$ indicates time average. There are two possible causes for the superdiffusion:

a) $D > 0$ and, in order to violate the condition (2.7), $\mathbf{u}$ with strong spatial correlation;

b) $D = 0$ and strong time correlation between $\mathbf{u}(\mathbf{x}(t))$ and $\mathbf{u}(\mathbf{x}(t+\tau))$ at large τ.

In the following sub-sections we present three different paradigmatic models showing anomalous diffusion originated by different mechanisms:

i) transport in incompressible random flows (Sect. 2.1.1) where the failure of the standard diffusion relies on the breakdown of hypothesis (2.7);

ii) diffusion in symplectic maps (Sect. 2.1.2) that represents a discrete version of transport process in 2D incompressible flows. In these system, the anomalous behaviour is a consequence of the strong correlations at large times enhanced by the presence of ballistic-like trajectories;

iii) relative dispersion of two particles in three-dimensional turbulence (Sect. 2.1.3), in which the Laplacian operator $\hat{L}$ is built by simple phenomenological arguments.

2.1.1 Random shear flow

One of the few non trivial systems for which the presence of anomalous diffusion can be proved rigorously is the $2D$ random shear flow. In this case, the transport dynamics is generated by the combined effects of the velocity field and the molecular diffusivity. Matheron and De Marsily [40] showed that anomalous diffusion, in the $x-$direction, occurs in a 2D random shear $\mathbf{u} = (u(y), 0)$, if the infrared contribution to $u(y)$ is strong enough to violate Eq. (2.7). For example the infrared ($k \sim 0$) divergence, $\langle |\hat{\mathbf{u}}(\mathbf{k})|^2 \rangle \sim k^\gamma$ entails for $\gamma \geq 1$ a diffusive asymptotic transport; instead, for $-1 \leq \gamma < 1$, the transport is asymptotically superdiffusive:

$$\langle |x(t) - x(0)|^2 \rangle \simeq t^{2\nu} \qquad \text{with} \qquad \nu = \frac{3-\gamma}{4} > 1/2\,. \tag{2.8}$$

The case $\gamma = 0$ has been studied in great details [11] and the PDF of a test particle around x at time t (starting with a distribution $P(x, 0)$

localized around $x = 0$) is

$$P(x,t) \sim \frac{1}{t^{3/4}} \exp\left[-C\left(\frac{|x|}{t^{3/4}}\right)^4\right] \tag{2.9}$$

where C is a constant.

2.1.2 Anomalous diffusion in chaotic symplectic systems

Anomalous diffusion has been observed in 2D laminar periodically time dependent incompressible flows [16]. In such a case, the Poincaré map technique shows that the motion of a fluid particle is described by a 2D symplectic map [33]. Therefore it is quite natural to study the diffusive behaviour of the standard map [33] which displays the typical features of low-dimensional Hamiltonian systems, whose dynamics is given by

$$\begin{cases} J_{t+1} &= J_t + K \sin\phi_t \\ \phi_{t+1} &= [\phi_t + J_{t+1}] \mod 2\pi\,. \end{cases} \tag{2.10}$$

As soon as $K > 0$ the system is not integrable and bounded chaotic regions appear. However, in order to have a fully developed diffusion in the variable J_t, K must be larger than $K_c \approx 0.97$. A very crude approximation, amounting to assume ϕ_t as a sequence of independent variables, gives

$$D_J^e \simeq \frac{K^2}{2}\langle \sin^2\phi\rangle = \frac{K^2}{4}\,. \tag{2.11}$$

A more precise argument [47], that is able to take into account the time correlation of ϕ_t is in good agreement with D_J^e values obtained by numerical computation for $K > 3$ with the exception of small regions around some specific values of K. Anomalous diffusion occurs for such specific values, where ballistic-like trajectories of J_t appear, known as accelerator modes, whose regular dynamics gives a non integrable contribution to the velocity-velocity correlation function and produces superdiffusion [54], [27], [38]. For instance at $K = 6.9115$, one observes $\nu \simeq 0.66$ and a non Gaussian shape of the $P(J,t)$ [16]. However, even for K-values admitting accelerator modes, the addition of a small noise to the dynamics makes the diffusion normal [34]. The noise term, indeed, avoids the stickiness to the accelerator modes.

2.1.3 Pair dispersion in fully developed turbulence

So far, we have considered the behaviour of a single particle, here we show that anomalous diffusion naturally arises even when studying the

two-particles properties of a fluid. Consider indeed the dispersion of a pair of particles advected by a homogeneous, isotropic, fully developed turbulent field. Such a problem is rather important in applications as it describes the spreading of pollutants in presence of turbulence.

Because of the incompressibility of the velocity field, the distance between the two particles will, on average, increases [18]. Richardson [48] proposed for the PDF, $P(\mathbf{r},t)$, of the two-particle separation $\mathbf{r}=\mathbf{r}_2-\mathbf{r}_1$, the following evolution equation in d dimensions

$$\partial_t P(\mathbf{r},t) = \left[\nabla\cdot(K(r)\nabla)\right] P(\mathbf{r},t)\,. \tag{2.12}$$

The effects of turbulence are taken into account in the turbulent diffusivity $K(r)$. From a collection of experimental data, Richardson [48] proposed his "4/3" law

$$K(r) = \alpha r^{4/3}\,.$$

It is easy to realize a posteriori that the above relation is a straightforward consequence of the Kolmogorov scaling [24]. Assuming isotropy, Eq. (2.12) can be written as

$$\partial_t P(r,t) = \frac{1}{r^{d-1}}\frac{\partial}{\partial r}\left(K(r)r^{d-1}\frac{\partial}{\partial r}P(r,t)\right)\,, \tag{2.13}$$

whose asymptotic solution is the non Gaussian PDF:

$$P(r,t) \sim \frac{1}{t^{3/2}}\exp\left[-C\left(\frac{r}{t^{3/2}}\right)^{2/3}\right]\,. \tag{2.14}$$

Thus, the growth law for the average separation between the particles is

$$\langle |r(t)|^q\rangle \sim t^{\nu q}\,, \tag{2.15}$$

with $\nu = 3/2$. In spite of its apparent simplicity, Richardson's approach is able to describe, in a quantitative way, the pair dispersion in synthetic turbulent fields [8] and in turbulent fields obtained by direct numerical simulations as well [9].

Moreover, Eq. (2.13) can be used to describe a rather general class of transport processes. As an example, we can mention the diffusion on fractal geometries of dimension $d_f = d$, where a radius-dependent diffusion coefficient $K(r) \propto r^\xi$ can be assumed [44].

The general solution corresponding to Eq. (2.13) with $K(r) \propto r^\xi$ is:

$$P(r,t) \sim \frac{1}{t^{\frac{1}{2-\xi}}}\exp\left[-C\left(\frac{r}{t^{\frac{1}{2-\xi}}}\right)^{2-\xi}\right]\,, \tag{2.16}$$

which extends formula (2.14). Therefore the "typical position" is $X_f \sim t^{\frac{1}{2-\xi}}$, and, changing ξ, we can explore subdiffusive ($\xi < 0$), normally diffusive ($\xi = 0$) and superdiffusive ($\xi > 0$) regimes.

2.2 Strong anomalous diffusion in stochastic processes

As we have seen before, in the presence of anomalous diffusion the PDF of the process is typically no longer Gaussian. A natural issue is to determine the shape of $P(x,t)$, at least for large times. A simple assumption, looking at Eqs. (2.13) and (2.9), is the scaling behaviour

$$P(x,t) \simeq t^{-\nu} F\left(\frac{|x|}{t^{\nu}}\right) . \tag{2.17}$$

The normal diffusion corresponds to $\nu = 1/2$ and $F(z) = \exp(-\mathrm{c}z^2)$. For $\nu \neq 1/2$, it has been proposed [11]

$$F(z) \propto e^{-c|z|^{\alpha}} . \tag{2.18}$$

One could hope that α is a function of ν only, but in general this is not true. Nevertheless, it is interesting to note that both Eqs. (2.17) and (2.18) are consistent with an argument á la Flory due to Fisher in the context of polymer physics [19] predicting:

$$P(x,t) \sim t^{-\nu} \exp\left[-c\left(\frac{|x|}{t^{\nu}}\right)^{\frac{1}{1-\nu}}\right] , \tag{2.19}$$

with $\alpha = 1/(1-\nu)$. We will see in the following that the shape (2.19) has an interesting consequence for the front propagation in reactive systems, since transport processes whose PDF scales like (2.19) give rise to a reactive-transport with constant propagation velocity. In general, when a reactive term is added to a transport-diffusion equation not only ν but also the exponent α is important to determine the front propagation features.

Let us remark that the scaling (2.17) implies

$$\langle |x(t)|^q \rangle \sim t^{q\nu}, \tag{2.20}$$

therefore, a single exponent is able to characterize the asymptotic behaviour of all the moments. We refer to this case as *weak* anomalous diffusion. However, certain deterministic and stochastic processes [29]

show that the simple scaling (2.20) is not always verified, and a more intricate scenario characterized by the generalized scaling

$$\langle |x(t)|^q \rangle \sim t^{q\nu(q)} \tag{2.21}$$

instead holds, where also the exponent $\nu = \nu(q)$ depends on q. This property is referred to as *strong anomalous diffusion* [16].

Remarkably strong anomalous diffusion is also present in apparently simple stochastic processes like some continuous time random walks (CTRW) [28], that are a variant of the classic random walk (RW), where a particle undergoes a series of kicks (collisions) at random times $t_1, t_2, \ldots, t_n, \ldots$ and between two consecutive collisions the velocity remains constant. The position of the particle at time t, such that $t_n < t \leq t_{n+1}$, will be

$$x(t) = x(t_n) + v_n(t - t_n) \tag{2.22}$$

and both the time intervals $\tau_n = t_{n+1} - t_n$ and the velocities v_n are independent random variables with arbitrary distribution [28]. In the following we consider a variant with a truncated power law distribution

$$P(\tau) \propto \begin{cases} \tau^{-g} & 1 \leq \tau \leq T \\ 0 & \text{elsewhere} \end{cases} \tag{2.23}$$

with $g > 1$ and $v_n = \pm 1$ with equal probability. The presence of the cutoff T implies that the hypothesis of the CLT for the process (2.22) are fulfilled, thus as $t \gg T$, it converges to a Gaussian process. However for T sufficiently large [39], the convergence can be made so slow that a long and robust pre-asymptotic regime of strong anomalous diffusion takes place.

A quantity that will be important in the following is the q-order moment of the waiting time τ whose asymptotic scaling for large T is the following

$$\langle \tau^q \rangle_c \sim \begin{cases} T^{1-g+q} & \text{if } q > g-1 \\ a(q,g) & \text{if } q < g-1 \end{cases} \tag{2.24}$$

where $a(q, g)$ is a constant independent of T and the index c indicates the average over the "truncated" distribution. At $T \to \infty$, various diffusive regimes occur depending on the value of the exponent g, see [4] and [22], in particular the case $g \in (3, 4]$ corresponds to the anomalous diffusion, $\langle |x(t)|^q \rangle \sim t^{q\nu(q)}$, with

$$q\nu(q) = \begin{cases} q/2, & q = 1, 2 \\ q + 2 - g, & q = 3, 4, 5, \cdots \end{cases} \tag{2.25}$$

The above behaviour of $q\nu(q)$ is quite peculiar as ,for $q \leq 2$, it corresponds to normal diffusion, while, for larger q, we have $q\nu(q) \neq q/2$, and this represents an example of strong anomalous regime.

The above behaviour of $q\nu(q)$ is quite peculiar as it coincides with that one of normal diffusion for $q \leq 2$, while for larger q, we have $q\nu(q) \neq q/2$, and this represents an example of strong anomalous regime. The relation (2.25) provides strong indications on the possible form of the PDF bulk; the lowest order moments behave in time as in the case of normal diffusion, thus we expect that the $P(x,t)$ has a Gaussian-like bulk which scales as $P(x,t) = t^{-1/2} f(xt^{-1/2}))$ for moderate values of the argument $|x/\sqrt{t}|$. The collapse of the rescaled PDF of the CTRW (2.22) at different times is shown in Figure 1.
It is worth remarking that the above result is not actually a violation of the CLT, as in the bulk all the PDFs collapse onto a Gaussian and only the tails deviate from it. The CLT, indeed, does not grant anything on the nature of the tails, it only specifies the shape of the limit distribution within the scaling region, $|x(t)/\sqrt{t}| \sim O(1)$. The tails outside such a region are not universal and generally not Gaussian.

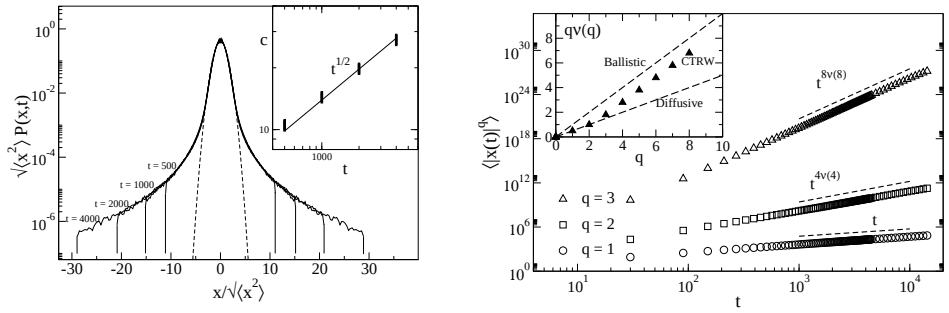

Figure 1: Statistical features of the CTRW process (2.22) and (2.23). On the left, rescaled probability densities at different times for $g = 3.2$. The vertical lines mark the truncated probability distribution at the bounded domain, $|x| \leq c(t)$, the dashed lines represents the Gaussian. The inset shows the scaling $c(t)/\sqrt{t} \sim t^{1/2}$ of the domain size. On the right, power law scaling of the moments with time, the inset reports the nonlinearity of $q\nu(q)$ as it defined in Eq. (2.25). Adapted from [22].

2.3 Diffusion on graphs

In this section we briefly discuss a transport process on the discrete structure of graphs. An undirected graph is a collection of vertices pairwise connected, or not, by links [10]. An $N \times N$ matrix, A, called adjacency matrix, can be associated to each graph of N-vertices's, with entries $A_{ij} = 1$ if there is a link between vertices's i and j, $A_{ij} = 0$ otherwise. A fundamental quantity is the degree of nodes, $k_i = \sum_j A_{ij}$, that measure the number of links established by each node $i \in [1..N]$.

An unbiased random walk on a graph can be defined whenever a walker at time t on the node i can jump at time $t+1$ on the node j with a transition probability A_{ij}/k_i. The latter assumption of equal-probability of the transition (possible only when $A_{ij} = 1$) to nearest neighbours of i can be relaxed by introducing some bias in the jump probabilities.

The diffusion properties of a random walk on graphs depend on both the *fractal dimension* [37] d_f, that is related to the scaling of the number of points in a sphere of radius ℓ: $N(\ell) \sim \ell^{d_f}$, and the *spectral dimension* d_s, that is defined by the return probability $q_t(x)$ to a generic site x in t steps $q_t(x) \sim t^{-d_s/2}$ [3]. In isotropic structures, the mean square displacement scales as (see [12] and [13])

$$\langle x^2(t) \rangle \sim t^{d_s/d_f}, \tag{2.26}$$

while, in anisotropic graphs, the above equation can fail (see [7] and [41]). The continuous-time diffusion on graphs [10] is ruled by the following master equation

$$\frac{\mathrm{d}P_i}{\mathrm{d}t} = D \sum_j W_{ij} P_j \tag{2.27}$$

where $W_{ij} = A_{ij} - k_i \delta_{ij}$ is the Laplacian on the graph and k_i is the degree of the node i. Given the graph properties one can wonder about the behaviour of high-order moments and the possible shape of the PDF.

Just to give an example of diffusion on graph, we consider the comb lattice in Fig. 2. The structure of the comb is such as sites $(n, 0)$, where $n = 0, \pm 1, \pm 2, \cdots$, define the backbone (horizontal line) of the graph, and the "teeth", i.e., sites (k_l, m), where $m = 0, \pm 1, \pm 2, \cdots$ and k_l labels the x-coordinate of the $l-$th "tooth" (in Fig. 2 $k_l = 5l$), gives the lateral escaping structures. Denoting by $P_{\mathbf{i}}(t)$ the probability to be on the site $\mathbf{i} = (n, m)$ at time t, the evolution equation is given

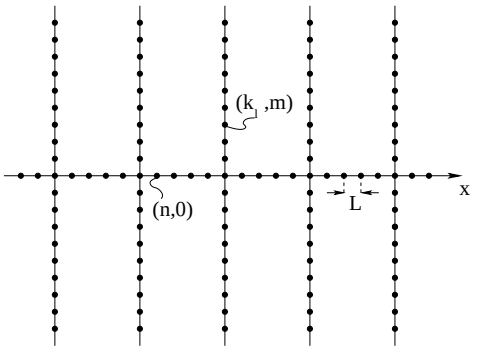

Figure 2: Representation of a comb lattice, as an example of a graph with a branched structure. Adapted from [36].

by (2.27), where A_{ij} is the adjacent matrix of the comb. Because of the possibility to "escape" along the vertical teeth, the diffusion process on the horizontal direction has a subdiffusive character [15],[21]:

$$\langle |x(t)|^2 \rangle \sim t^{1/2} \qquad \text{i.e.} \qquad \nu = 1/4\,. \tag{2.28}$$

Numerical simulations [36] show that the PDF $P(x,t)$ behaves like

$$P(x,t) \sim \frac{1}{t^{1/4}} \exp\left[-C \left(\frac{|x|}{t^{1/4}} \right)^{4/3} \right] , \tag{2.29}$$

and it is worth to note that in this case the Fisher's conjecture (2.19) holds.

2.3.1 Normal diffusion on fractal graphs

Consider now the diffusion in a special class of graphs the *Nice Trees of dimension k* (NT_k) that are recursively defined from an origin $\mathcal{O}$ as it is described in Fig. 3. Such trees are characterized by the remarkable property that fractal and spectral dimension coincide [12] and [13],

$$d_f = d_s(k) = 1 + \frac{\ln k}{\ln 2} \tag{2.30}$$

therefore, despite the nontrivial structure, Eq. (2.26) implies a normal behaviour $\langle x^2(t) \rangle \sim t$ for any values of k. However, the linear growth of the mean square displacement in time (i.e. $2\nu(2) = 1$) does not necessarily imply a Gaussian diffusive behaviour. Therefore to fully characterize the diffusion properties of the unbiased random walk on the NT_k, we need to determine the probability distribution that a

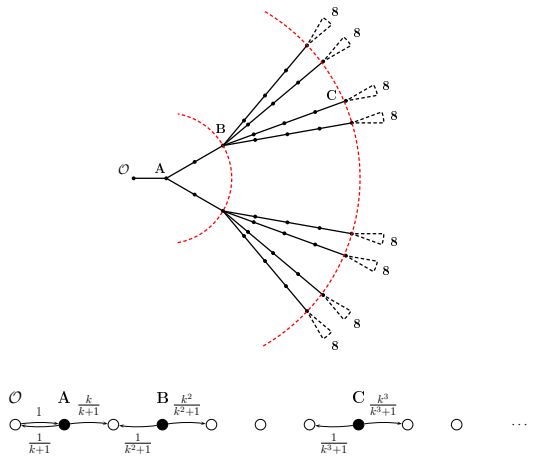

Figure 3: Geometrical construction of a Nice Tree of dimension $k = 3$. The origin $\mathcal{O}$ is connected with a point A by a link of length 1; from A the tree splits in k branches of length 2^1 each. The end point of such branches, in turn, splits again into k branches of length 2^2 and so on. Below, the transition rules for a walker to be one step closer or farther to the origin $\mathcal{O}$, full dots mark the branching points. Adapted from [22].

walker lays at distance x from the origin $\mathcal{O}$. To this purpose, we assign to the site the integer distance x if it is connected to $\mathcal{O}$ by a minimal path with x-links. It is remarkable that the projected process obtained by using the new variable x still maintains the Markov properties and it is ruled by the following (discrete time) master equation [22]:

$$\begin{aligned} P_{t+1}(x-1) = &\quad \frac{1}{2}P_t(x-2) + \frac{1}{k+1}P_t(x) \\ P_{t+1}(x) = &\quad \frac{1}{2}P_t(x-1) + \frac{1}{2}P_t(x+1) \\ P_{t+1}(x+1) = &\quad \frac{k}{k+1}P_t(x) + \frac{1}{2}P_t(x+2) \end{aligned} \tag{2.31}$$

where, with reference to Fig. 3, the first and third equations holds only for branching points ($x = 2^n - 1$), the second one for all the other sites. Accordingly, the transition matrix $w(x \pm 1|x)$ of the one-dimensional RW from $x \to x \pm 1$, in a time step reads

$$w(x+1|x) = \begin{cases} \dfrac{k}{k+1}, & \text{if } \; x = 2^n - 1 \\ 1/2, & \text{elsewhere} \end{cases} \tag{2.32}$$

$$w(x-1|x) = \begin{cases} \dfrac{1}{k+1}, & \text{if } x = 2^n - 1 \\ 1/2, & \text{elsewhere} \end{cases} \tag{2.33}$$

where $2^n - 1$ is the formula identifying the distance of the branching points from the origin $\mathcal{O}$, $W(1|0) = 1$ is the condition for a reflecting boundary in $\mathcal{O}$. The RW on NT_k is thus mapped onto a RW on a one-dimensional lattice in a deterministic heterogeneous environment. The physical interpretation of the transition rules are straightforward: if a walker stays on a branching point, there are k possibilities to go one step away from origin and 1 possibility to make one step closer. Then the next step will take it either farther from the origin with probability $p_+ = k/(k+1)$ or closer the origin with probability $p_- = 1/(k+1)$. Whereas if a walker is outside the branching point, both steps are unbiased, $p_- = p_- = 1/2$. The inhomogeneity stems from the branching points $x = 2^n - 1,\ n = 1, 2, 3 \cdots$ which represent special points ("defects") but become exponentially rare as long as the walker lies far away from the origin. Thus, far away from the origin, the process remains an unbiased RW for so long time that "Gaussian character" of the distribution is not altered by the presence of defects.

Figure 4 shows the simulation results for the probability density $P_t(x)$ rescaled to $x \to x/\sqrt{\langle x^2 \rangle}$ and $P_t(x) \to \sqrt{\langle x^2 \rangle} P_t(x)$ obtained by iterating the master equation (2.31) for NT_k with $k = 2$. The dash-dotted curve is the approximated solution

$$F_t(x) = \frac{2x^{d_s - 1}}{\Gamma(d_s/2)(2t)^{d_s/2}} \exp(-x^2/2t) \tag{2.34}$$

which well interpolates the exact numerical result. Expression (2.34) is the radial Gaussian distribution in dimension $d_s(k)$

As a final remark we note that, despite the geometrical complexity of NTk, the large scale statistical properties of RW on this graph remains Gaussian-like, as, on the other hand, it expected by the shape of the approximated distribution (2.34).

3 Front propagation in reactive transport systems with anomalous diffusion

In the previous Section, different mechanisms for anomalous diffusion, corresponding to suitable transport operators $\hat{L}$, have been discussed. Here we consider systems where anomalous diffusion is coupled to a

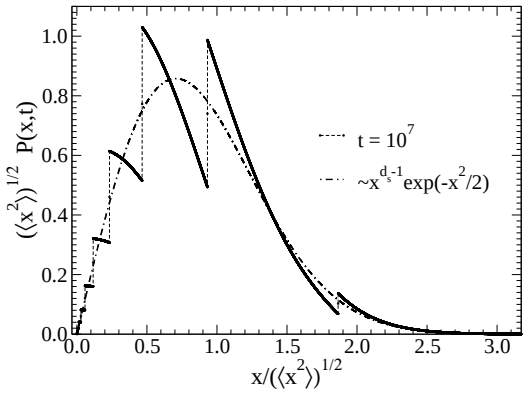

Figure 4: Probability density obtained by iterating the master equation (2.31) for a NT_k with $k = 2$. Dashed line indicates the interpolation with the Gaussian radial distribution in dimension d_s. Adapted from [22].

reaction dynamics leading to a generalized reaction diffusion equation

$$\frac{\partial \theta}{\partial t} = \hat{L}\theta + \frac{1}{\tau} f(\theta) \tag{3.1}$$

whose solution can be compared with the classical theoretical framework corresponding to the FKPP Equation (1.5). In particular, we focus on the asymptotic features of front propagation generated by Eq. (3.1).

We recall that the FKPP equation admits propagating fronts separating regions with $\theta \simeq 1$ and $\theta \simeq 0$. The standard propagation scenario is then defined by a constant front speed $v_f = 2\sqrt{D_0 f'(0)/\tau}$ (see [20] and [32]) with a thickness of the front given by $\xi = 8\sqrt{D\tau/f'(0)}$ and an exponential decay of θ at large x

$$\theta(x,t) = F(x - v_f t) \qquad \text{with} \qquad F(z) \sim e^{-z/\xi} \quad \text{for} \quad z \gg 1\,. \tag{3.2}$$

When dealing with Eq.(3.1) a question naturally arises about the conditions needed to change the FKPP propagation scenario. We will see that if the transport operator $\hat{L}$ at large time exhibits a normal diffusion behaviour and the reaction time τ is large enough, then a standard propagation scenario establishes. However, the presence of anomalous diffusion alone it is not sufficient to guarantee an anomalous transport [52], i.e. a non constant front speed. We will see that for the reaction spreading is relevant not only the anomalous exponent ν but the details of the mechanism play a major role. This can be explicitly shown for some cases, see [35] and [36] for details.

Studying different reacting systems in the presence of anomalous diffusion, we discuss 3 different scenarios:

a) exponential decay of θ with constant front speed v_f and thickness ξ, i.e. Eq. (3.2);

b) exponential decay of θ but v_f and ξ can vary in time as a power law;

c) power law decay of $\theta(\mathbf{x},t) \sim |x - v_f t|^{-\alpha}$ and v_f exponentially increases in time.

3.1 Some general results

Consider the case in which the generalized diffusion equation (2.2) generates asymptotically normal diffusion. It is possible to prove [23] a relation between the solution of Eq. (3.1) and the Lagrangian trajectories $\mathbf{x}(t)$ associated to the diffusion process (2.2):

$$\theta(\mathbf{x},t) = \left\langle \theta(\mathbf{x}(0),0)\, \exp\left(\frac{1}{\tau}\int_0^t \frac{f(\theta(\mathbf{x}(s;t),s))}{\theta(\mathbf{x}(s;t),s)}\mathrm{d}s\right)\right\rangle , \qquad (3.3)$$

where the average is performed over all the trajectories $\mathbf{x}(s;t)$ that started in $\mathbf{x}(0)$ and ended in $\mathbf{x}(t;t) = \mathbf{x}$. Equation (3.3), although rather important from a theoretical point of view, cannot be easily used for explicit computations. However it suggests the implementation of an efficient stochastic algorithm for numerical simulation of the Eq. (3.1) (see [1]). In addition, using the maximum principle [23] and noting that, because of the convexity of $f(\theta)$, $f(\theta)/\theta \leq f'(0)$ one can write an upper bound for θ in terms of the solution of the linearized Eq. (3.1):

$$\partial_t \theta_L = \hat{L}\theta_L + \frac{f'(0)}{\tau}\theta_L \, . \qquad (3.4)$$

In fact, if $\theta(\mathbf{x},0) \leq \theta_L(\mathbf{x},0)$ the maximum principle [23] implies

$$\theta(\mathbf{x},t) \leq \theta_L(\mathbf{x},t) \qquad (3.5)$$

for all times. From Eq.s (3.3-3.5) one obtains

$$\theta(\mathbf{x},t) \leq \theta_L(\mathbf{x},t) = \langle \theta(\mathbf{x}(0;t),0)\rangle \exp\left(\frac{f'(0)}{\tau}t\right) , \qquad (3.6)$$

where $\langle \theta(\mathbf{x}(0;t),0)\rangle = P(\mathbf{x},t)$ is the solution of Eq. (2.2) with initial condition $\theta(\mathbf{x},0)$ (that we assume localized around $\mathbf{x} = 0$). In the Introduction and in Sect. 2, we saw that under general conditions

(i.e., spatial and temporal short-range correlations) Eq. (2.2) has the same asymptotic behaviour of a Fick equation. As a consequence (see also Eq. (1.4)), we have

$$\langle \theta(\mathbf{x}(0;t),0)\rangle \sim \exp\left\{ -\frac{1}{4t}\sum_{i,j} x_i \left[D^e\right]^{-1}_{ij} x_j \right\} . \tag{3.7}$$

Eq.s (3.6) and (3.7) imply that, along the x-direction, the field θ is exponentially small until a time t of the order of $x/\sqrt{4D^e_{11}f'(0)/\tau}$. Therefore, considering just 1D propagation along the x direction, we have an upper bound for v_f

$$v_f \leq 2\sqrt{D^e_{11}f'(0)/\tau}\,. \tag{3.8}$$

The above discussion shows that, if normal diffusion holds, there is a front propagating with a constant finite speed. Nevertheless, the analytical determination of v_f is rather difficult even for simple laminar fields [1].

3.2 Behaviour of the front position

Let us now give an argument for the front propagation in systems with anomalous diffusion. As previously discussed a simple linear analysis, using the Feynman-Kac like formula (3.3) and the maximum principle, leads to Eq. (3.6), here rewritten as

$$\theta(x,t) \leq P(x,t)\, e^{\,ct},$$

where $c = f'(0)/\tau$. When the scaling law (2.17) together with Eq. (2.18) holds, the following relation applies

$$\theta(x,t) \leq t^{-\nu}\, F\left(\frac{|x|}{t^\nu}\right)\, e^{ct} \;\sim\; t^{-\nu}\, \exp\left[-C\left(\frac{|x|}{t^\nu}\right)^{\alpha} + ct\right] . \tag{3.9}$$

Imposing $\theta(X_f(t),t) \sim 1$, where $X_f(t)$ is the front position, it follows from the previous bound $\theta \lesssim e^{-C(X_f t^{-\nu})^\alpha}\; e^{ct} \sim 1$ and therefore one has

$$X_f(t) \sim t^\gamma \quad \text{with} \quad \gamma = \nu + \frac{1}{\alpha}\,. \tag{3.10}$$

In all numerical computations we always observe $X_f \sim t^\gamma$, since for convex reaction terms the front is pulled by perturbations of the unstable state, whose evolution is given by the linearized problem. Note that γ depends not only on ν but also on α. However, if the Fisher's

argument of Eq. (2.19) holds, i.e. if $\alpha = 1/(1-\nu)$, we have $\gamma = 1$. That is, despite the presence of anomalous diffusion, the FKPP front propagation scenario remains valid. For example we can consider two different cases, one of subdiffusion (comb lattice) and another of superdiffusion (random shear flow) both in the Flory class and, in both, the front propagation is standard. Fig. 5 shows front propagation in the comb lattice.

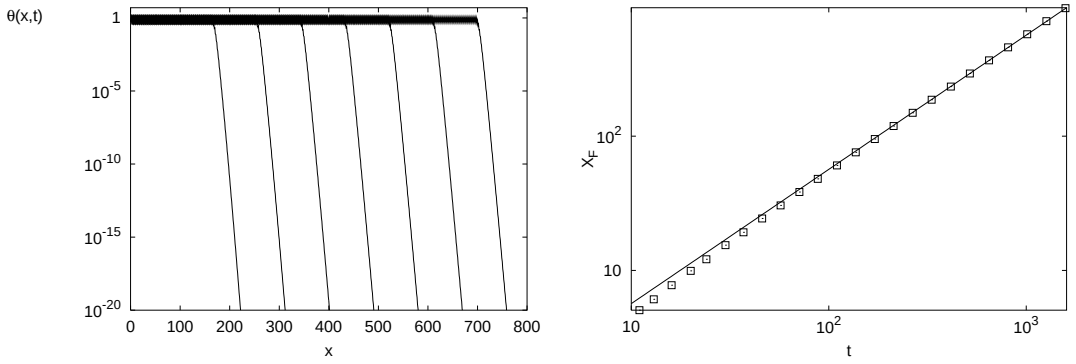

Figure 5: Front propagation (on the left) and typical front position X_f (on the right) for the reaction dynamics on a comb lattice. The solid line displays a linear behaviour. Adapted from [36].

In order to find the shape of the front, we study Eq. (3.9) around the typical position $X_f \sim t^\gamma$. In fact, introducing the displacement $\eta = x - X_f$, it results $\theta \sim \exp\left[-\alpha C t^{-(\nu\alpha-\gamma(\alpha-1))}\eta + o(\eta^2)\right]$. As $\gamma = \nu + 1/\alpha$ (see Eq. (3.10)), $\theta \sim \exp\left[-\alpha C t^{1-\gamma}\eta + o(\eta^2)\right]$.
Summarizing, the typical position of the front grows as $X_f \sim t^\gamma$ (3.10) and the shape of $\theta(x,t)$ around X_f is

$$\theta(x,t) \sim \exp\left[-\frac{x - X_f(t)}{\xi(t)}\right] \quad \text{with} \quad \xi(t) \sim t^\delta \quad \text{and} \quad \delta = \gamma - 1 \ . \tag{3.11}$$

This implies, for instance, that in all the cases in which we observe linear propagation of the front ($\gamma = 1$), we also have a constant front thickness ($\delta = 0$), just as in the FKPP equation. In general, the above scenario remains valid also in the presence of other anomalous diffusion processes providing that $P(x,t)$ be of the form Eq. (2.17) together with Eq. (2.18). Conversely, if Eq. (2.17) or Eq. (2.18) is no more satisfied, and different propagation behaviour are allowed (see [35] and [36]).

3.2.1 Generalized Richardson diffusion

It is instructive to apply the above analysis to a system whose transport process is given by the Richardson diffusion equation (as in Eq. (2.13)), with the asymptotic solution given by (2.14). It is important to note that this is not the case of a Flory shape (2.19). We also recall that the growth law for the average separation between the particles is $\langle |r(t)|^2 \rangle \sim t^3$.

The simplest way to study the reaction transport problem for fully developed 3D turbulence is to consider Eq. (3.1) with the transport operator $\hat{L}$ given by Eq. (2.13), i.e.:

$$\partial_t \theta(r,t) = \frac{1}{r^{d-1}} \frac{\partial}{\partial r} \left(K(r) r^{d-1} \frac{\partial}{\partial r} \theta(r,t) \right) + \frac{1}{\tau} f(\theta) \,. \tag{3.12}$$

In Eq. (3.12) $r = 0$ indicates the center of the spot. One can wonder about the validity of (3.12) as a reasonable model for reaction process in turbulent field. It is known that, in systems with normal diffusion, for slow reaction, i.e., $\tau \gg L/U$, the large scale and long time asymptotic of the reaction advection diffusion equation $\partial_t \theta + \mathbf{u} \cdot \nabla \theta = D \Delta \theta + f(\theta)/\tau$ is well approximated by a reaction diffusion equation with eddy diffusivity tensor D^e of the corresponding problem (1.2), i.e., $v_f \simeq 2\sqrt{D^e_{11} f'(0)/\tau}$ [1]. On the base of this result one can expect that Eq. (3.12) is a suitable approximation if τ is larger than the eddy turnover times in the inertial range. This condition, hardly satisfied in chemical context, has its relevance in ecological problems where equations similar to (3.12) are considered [45].

Figure 6 shows the propagation and the typical position of the front. It is apparent the good agreement between numerical results and theoretical prediction of Eq. (3.10). In the inset of the right panel of Fig. 6 the front thickness appears to be time dependent according to the prediction of Eq. (3.11), i.e., the front shape changes as the front propagates. We remind that the standard propagation is characterized by a rigid translation of the front (e.g., see Eq. (3.2)).

3.2.2 Diffusion processes with power law tails

It is also interesting to investigate reaction processes in the case of diffusion dynamics with power law tails. As an example we consider the Lévy flight which follows the rule

$$x(t+h) = x(t) + h v(t) \tag{3.13}$$

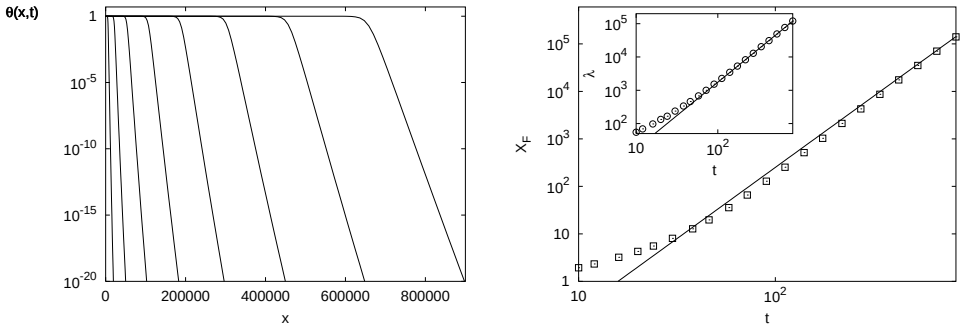

Figure 6: Propagation features of reactive fronts with Richardson diffusion in the case $K(r) = r^{4/3}$, $f(\theta) = \theta(1-\theta)$ and $\tau = 1$. On the left, front shape at different times. On the right typical position of the front X_f vs t. The full line indicates the theoretical prediction Eq. (3.10) with $\nu = 3/2$ and $\alpha = 2/3$. The inset shows the front thickness ξ together its theoretical prediction Eq. (3.11). Adapted from [36].

and $v(t)$'s are independent identically distributed (i.i.d.) random variables with a PDF decaying as a power law:

$$P_\alpha(v) \sim |v|^{-(1+\alpha)} \qquad \text{for } |v| \gg 1\,, \tag{3.14}$$

If $0 < \alpha < 2$, $v(t)$'s are in the basin of attraction of the α-Lévy stable distribution. Since $\langle v^2 \rangle = \infty$, one has $\langle |x(t)|^2 \rangle = \infty$. However introducing smaller moments $\langle |x(t)|^q \rangle = C_q t^{q/\alpha}$ with $q < \alpha$, a typical position $X_f = \sqrt[q]{\langle |x(t)|^q \rangle}$ can be defined, which grows as t^ν with $\nu = 1/\alpha > 1/2$. This process, called Lévy flight, is, therefore, superdiffusive.

Let us consider the reaction diffusion (3.1) where $\hat{L}$ corresponds to the process (3.13). Only for simplicity in the notation and in the numerical computation [1], we take into account a reacting term which is non zero only at discrete time step, when δ-form impulses occur:

$$f(\theta, t) = \sum_{n=-\infty}^{\infty} g(\theta)\delta(t - nh)\, h\ . \tag{3.15}$$

So between 0 and 0^+ Eq. (3.1) can be easily integrated: $\theta(x, 0^+) = G(\theta(x, 0))$ where $G(\theta) = \theta + \frac{h}{\tau} g(\theta)$. Then, between 0^+ and h, Eq. (3.1) reduces to the linear equation $\partial_t \theta = \hat{L}\theta$, and we can compute $\theta(x, h)$:

$$\theta(x,h) = \int_{-\infty}^{+\infty} \mathrm{d}w P_\alpha(w)\theta(x-w, 0^+) = \int_{-\infty}^{+\infty} \mathrm{d}w P_\alpha(w) G(\theta(x-w, 0))\,. \tag{3.16}$$

Iterating the previous procedure we can get $\theta(x,t)$, with $t = nh$. Let us note that Eq. (3.16) is exact only when Eq. (3.15) holds, while it is a good approximation when $f(\theta)$ is not a δ-impulsed function as long as h is small. In any case we are interested in pulled reactions (we recall that "pulled reactions" means $G''(\theta) > 0$ and $G'(0) > 1$). For this family of reactions the detailed shape of $G(\theta)$ is not important [1]. Numerical results obtained integrating Eq. (3.16), is shown in Fig. 7.

Note that X_f grows exponentially fast in time, and $\theta(x,t)$ develops

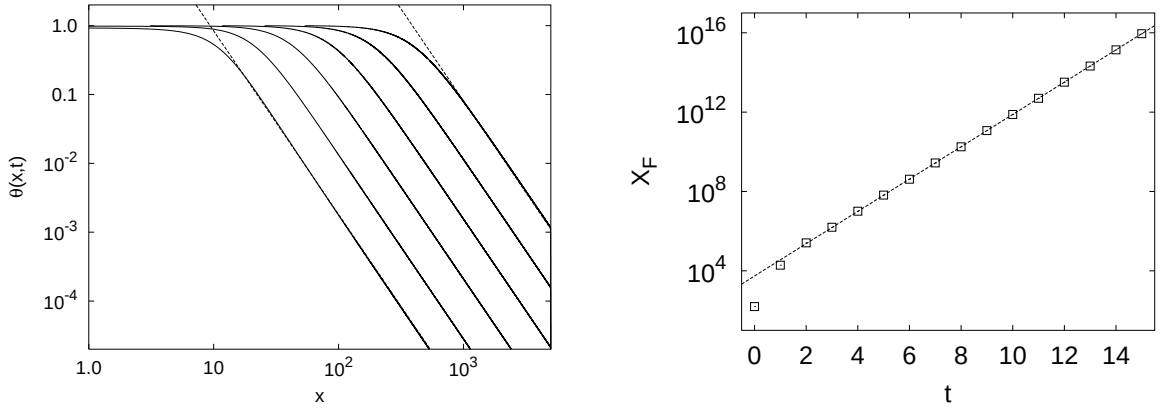

Figure 7: Front shapes at increasing times in the case of $P(w) \sim |w|^{-(1+\alpha)}$ with $\alpha = \frac{5}{3}$ and $G(\theta) = \theta + \frac{h}{\tau} g(\theta)$ with $\tau = 1$ (left). The dashed lines indicate the theoretical prediction $x^{-(1+\alpha)}$. On the right it is shown the exponential growth of the typical front position X_f and its asymptotic behaviour proportional to $a^{t/(1+\alpha)}$, with $a = G'(0)$ (right). Adapted from [35].

a power law tail for $|x| \to \infty$. The results shown in Fig. 7 can be supported by an analytical argument (very similar to the one used for diffusion process with exponential law tail PDF) via a linear analysis, which is expected to be valid in the FKPP reaction case, and the theory of the infinitely divisible distributions. For θ around zero, $G'(\theta)$ has a linear shape, $G'(\theta) \simeq a\theta$ with $a > 1$. Plugging this into Eq. (3.16) for $x \gg 1$

$$\theta(x,t) \simeq a\,(P_\alpha * \theta)(x, t-1) \simeq a^t\,(P_\alpha * P_\alpha * \cdots \theta)(x,0)\ , \qquad (3.17)$$

where, for the sake of notation simplicity, we assumed $h = 1$ (this corresponds to a rescaling of the time) and the symbol "*" indicates the convolution operator and P_α is the probability distribution for a single jump, that is in the basin of attraction of the α-Lévy stable

distribution, giving for $x \gg 1$ and large t:

$$\theta(x,t) \sim |x|^{-(1+\alpha)}\, a^t \ ,$$

which predicts the power law tail behaviour of the front shape. Then, X_f can be determined using $\theta(X_f(t),t) \sim 1$, which gives

$$X_f \simeq a^{\left[\frac{t}{1+\alpha}\right]} \ . \tag{3.18}$$

Now we wonder what happens if the distribution P_α has a power law tail but it belongs to the basin of attraction of a Gaussian PDF, i.e., if $\alpha \geq 2$.
At a first glance, since the diffusion is normal, one could expect the same features of the FKPP equation. Numerical results of Fig. 8 show a rather different scenario. For each localized initial condition, $\theta_0(x,t)$, already at the first step, the front has a shape not steep enough to allow the usual FKPP propagation. In fact, because of the reaction, the tail of θ increases exponentially in time. As a consequence of the Gaussian core of $P(x,t)$, we expect that the bulk of θ behaves in the FKPP way, but, at large time, the exponential growth of the tail has the dominant role, see [35] for a more detailed discussion. Fig. 8 shows how the exponential form of the front, initially moving with a constant velocity, is overcome by a power law tail that grows more and more as time increases. In other words, the initial FKPP behaviour (constant v_f and $\theta(x,t)$ with exponential decay) is replaced by the exponential increasing of the inert material and $\theta(x,t)$ with a power law tail.

4 Reaction diffusion on graphs: relevance of topology

In Sec. 2.3 we discussed the diffusion processes on graphs. It is natural to introduce here a reaction term in the diffusion equation on graphs (2.27):

$$\frac{d\theta_i}{dt} = \sum_j W_{ij}\theta_j + \frac{1}{\tau} f(\theta_i) \tag{4.1}$$

where the time has been rescaled to have a unique characteristic time: τ. We recall that $W_{ij} = A_{ij} - k_i\delta_{ij}$ is the Laplacian on the graph, and k_i is degree of the node i.

A common way to study the spreading of the reaction on a graph is to consider an initial concentration $\{\theta_i\}$ which is zero apart a small set of neighbours nodes, and look at the time course of the percentage

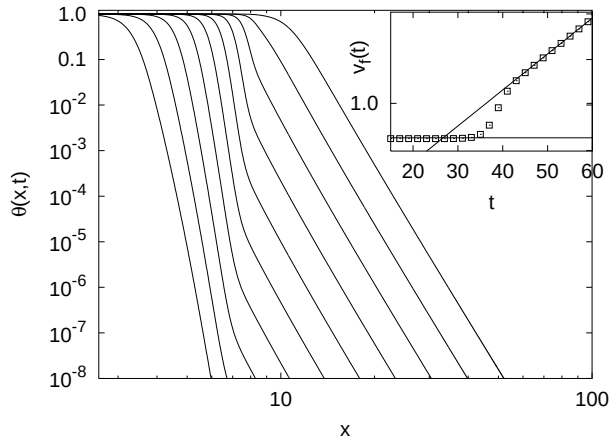

Figure 8: Front shapes at $t = 19, 22, 25 \cdots$ where $P(w)$ is the basin of attraction of $P_\alpha(w) \sim |w|^{-(1+\alpha)}$ with $\alpha = 10$. The inset shows the front speed $v_f(t) = X_f(t+1) - X_f(t)$. At short time, v_f is constant as in the FKPP propagation, whereas at longer time, the exponential propagation regime, $v_f \propto a^{\left[\frac{t}{1+\alpha}\right]}$, takes place. Adapted from [35].

of the reaction products $M(t) = \frac{1}{N}\sum_{i=1}^{N} \theta_i(t)$. Of course, in the case of a regular lattice (e.g. square) with dimension $d = 1, 2$ or 3 one has

$$M(t) = \frac{1}{N}\sum_{i=1}^{N} \theta_i(t) \sim t^d \ , \tag{4.2}$$

corresponding to a linear growth in a d-dimensional space of the initial condition. Let us wonder how the previous scaling is modified in a reaction-diffusion process on graph.

4.1 Reaction on geometrical graphs

In a geometric graph, i.e. a graph in which each vertex is a point in a space equipped with a metric, we expect that Eq. (4.2) is still valid but with a different d that is not so obvious to identify. In Sec. 2.3 we introduced the fractal dimension d_f and the spectral dimension d_s, two quantities that determine the scaling for the (typically anomalous) diffusion $\langle x^2(t)\rangle \sim t^{d_s/d_f}$ with $d_s/d_f \leq 1$ (see Eq. (2.26)). Detailed numerical simulations [14] on several graphs show

$$M(t) \sim t^{d_l} \tag{4.3}$$

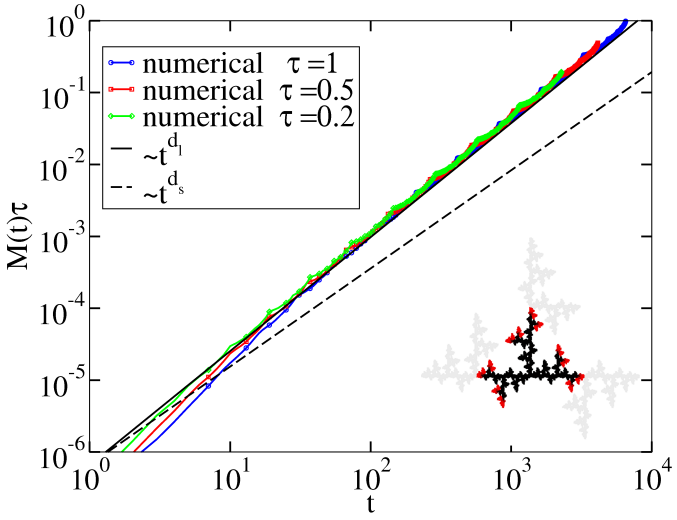

Figure 9: The percentage of quantity of product times τ, $M(t)\tau$ vs t. Numerical results for Eq. (4.1) are compared to prediction t^{d_l} and t^{d_s} in order to show that, definitively, the spreading follows the connectivity dimension. In the inset there is a graphical representation of the spreading on a T-graph: the black part is burned material ($\theta = 1$) while the grey is the fresh one ($\theta = 0$). Adapted from [14].

where d_l is the connectivity dimension (also known as "chemical dimension") that measures the average number of vertices connected to a vertex in at most l link, as $\#(l) \sim l^{d_l}$. As an example in Fig. 9 it is shown the scaling (4.3) for the T-graph for different reaction times τ. A T-graph is a fractal generated by iterating a rule which replaces a segment with a T-structure (from "—" to "⊤", see Fig. 1 of ref. [2]). An easy way to validate such a behaviour is the following. Denote with S_n the number of distinct sites visited by n independent random walkers, starting from the site 0, after t steps

$$S_n(t) = \sum_{j=0}^{N} (1 - C_{0j}(t)^n)$$

where $C_{0j}(t)$ is the probability that a walker starting from site 0 has not visited site j at time t. When the number of walkers is large ($n \to \infty$), $C_{0j}(t)^n$ tends to zero if site j has a nonzero probability of being reached in t steps. In this limit, $S_n(t)$ represents all the sites which have nonzero probability of being visited in t steps and, $S_n(t) \sim t^{d_l}$. This is precisely the regime observed in the reaction

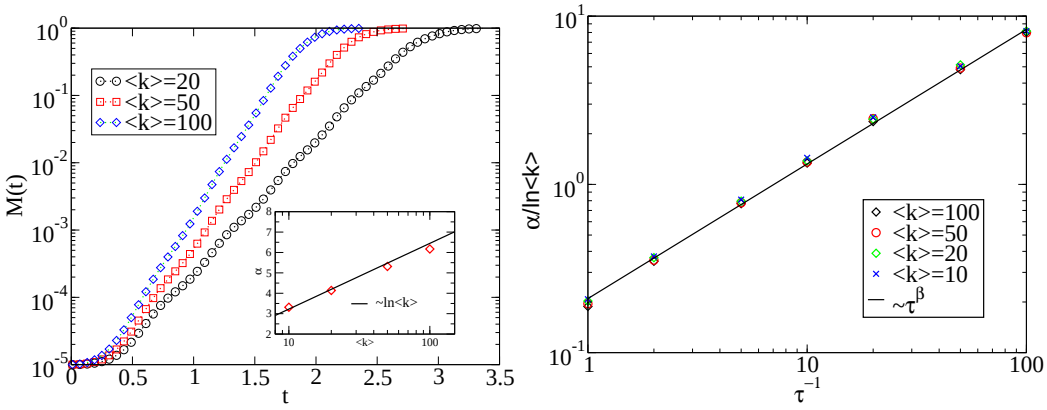

Figure 10: Reaction process Erdös-Renyi graphs. On the left it is reported $M(t)$ vs t for three different average degree of connectivity. The reaction spreading follows an exponential behaviour $M(t) \sim e^{\alpha t}$, where α depends on $\langle k \rangle$ as shown in the inset. On the right the scaling exponent α normalized with $\ln\langle k \rangle$, as a function of the inverse of reaction-time $\frac{1}{\tau}$, is reported. The straight line indicate τ^{β} with $\beta = -0.8$. Adapted from [14].

spreading.

Let us note that the result (4.3) is another way to understand the standard front propagation in the comb lattice discussed in Sect. 2.3. It is easy to realize that for such a graph $d_l = 2$, therefore, in spite of the non homogeneous spatial structure, the spreading of the reactive material has the same scaling law than that of a simple regular $2D$ lattice.

4.2 Reaction on Erdös-Renyi graphs

Let us now briefly discuss the spreading of the reaction on an important class of graphs: the Erdös-Renyi (ER) graphs [10] characterized by $d_l = \infty$. In the ER graphs with N vertices, two vertices are connected with probability p and the average degree of the graph connectivity is $\langle k \rangle = p(N-1)$. If $p > \ln(N)/N$ the graph contains a global connected component [10]. On ER graphs the number of points in a sphere of radius l grows exponentially, $N(l) \sim e^{cl}$, hence we expect a similar behaviour for the spreading process:

$$M(t) \sim e^{\alpha t}$$

as shown in the left panel of Fig. 10

If $\langle k \rangle$ is large and the reaction is slow enough we observe a two-step mechanism: first there is a rapid diffusion on the whole graph, then the reaction induces an increase of θ_i. This leads to a simple mean-field reaction dynamics, $d\rho/dt = \rho(1-\rho)/\tau$, where ρ is the average value of θ_i on the graph. In this case $\alpha = 1/\tau$ as clearly observed in numerical simulations (not shown here). In the much more interesting case of a fast reaction, at each time step the number of sites invaded is proportional to the average degree of the graph, so that after t steps we have

$$M(t) \sim (C_1\langle k \rangle)^t = e^{C_2 \ln\langle k \rangle t}$$

leading to $\alpha \sim \ln\langle k \rangle$, see the inset in the left panel of Fig. 10. Furthermore, at variance with the case of graphs with finite d_l, in the case of fast reaction and FKPP reaction term, τ plays an important role since C_2 is a function of τ, see [14]:

$$\alpha \simeq C\tau^{\beta} \ln\langle k \rangle$$

with $\beta \simeq -0.8$, as showed in the right panel of Figure 10.

5 Conclusions

Reaction-diffusion equations describe systems where the interplay between transport and reactions processes produces spatio-temporal variations on species concentrations.

The simplest situation occurs when the transport process follows the Fick's law and an autocatalytic term accounts for the reaction process. This is the reference case, also called FKPP dynamics, which admits travelling wave solutions with a constant speed.

However, in certain contexts, such as complex fluids, crowded environments or constrained geometries, the transport process cannot be described by a Fick's law, and the concentration of the reaction-free problem can undergo anomalous diffusion, i.e. $\langle |\mathbf{x}(t) - \mathbf{x}(0)|^2 \rangle \sim t^{2\nu}$ with $\nu \neq 1/2$.

Accordingly, the PDF is no more Gaussian and one can conjecture that a simple scaling hypothesis:

$$P(x,t) \sim t^{-\nu} F\Big(\frac{|x|}{t^{\nu}}\Big) \tag{5.1}$$

can be still verified. However the above scenario, called *weak* anomalous diffusion, is not always valid. Indeed, there exist more complex situations, the so called *strong* anomalous diffusion, that cannot be

characterized by a single exponent ν because the moments present multiscaling: $\langle |\mathbf{x}(t) - \mathbf{x}(0)|^q \rangle \sim t^{q\nu(q)}$, where $\nu(q)$ is a non constant function, and a full spectrum of exponents is required.

In this paper first we analyzed few basic mechanisms leading to anomalous diffusion (both in the weak or strong version). In particular, we focused on those cases in which the anomaly can be a consequence of: i) the peculiar properties of advecting fields; or ii) specific characteristic of stochastic processes; or finally iii) the confinement of the random walks on graph-like structures. Then we have seen how anomalous behaviour affects the reaction-diffusion process and changes the front propagation dynamics with respect to the reference case of the FKPP equation.

A linear analysis on the reaction-transport equation shows that, remarkably, if the PDF of the concentration of the reaction free problem satisfies the Flory scaling, that is $F(z) = \exp(-c|z|^\alpha)$ with $\alpha = 1/(1-\nu)$, the FKPP scenario still survives. Whereas, if the previous scaling is violated the front behaviour depends on the shape of the tails of the PDF, and not only on the value ν (even if $\nu = 1/2$). Remarkably we have the counterintuitive result that the front propagation could be faster than linear also in the case in which $\langle |\mathbf{x}(t) - \mathbf{x}(0)|^2 \rangle \sim t$.
Finally we considered the spreading of reactants on a graph. Although the diffusion on graphs is ruled by the ratio between the fractal and the spectral dimension, the growth of the percentage of the reaction products on the graph is determined by a unique exponent, i.e. the connectivity dimension d_l, $M(t) \sim t^{d_l}$. In the case of random (Erdös-Renyi) graphs, where formally $d_l = \infty$, we showed an exponential growth characterized by the average degree of the graph connectivity.

References

[1] M. Abel, A. Celani, D. Vergni and A. Vulpiani, *Front propagation in laminar flows*, Phys. Rev. E, 64 (2001), 046307.

[2] E. Agliari, *Exact mean first-passage time on the T-graph*, Phys. Rev. E, 77 (2008), 011128.

[3] S. Alexander, R. Orbach. *Density of states on fractals: fractons.* J. Phys. Lett., 43 (1982), 625–631.

[4] K. Andersen, P. Castiglione, A. Mazzino, A. Vulpiani. *Simple stochastic models showing strong anomalous diffusion.* Eur. Phys. J., B 18 (2000), 447–452.

[5] M. Avellaneda and A.J. Majda. *An integral-representation and bounds on the effective diffusivity in passive advection by laminar and turbulent flows*. Commun. Math. Phys., 138 (1991), 339–391.

[6] M. Avellaneda and M. Vergassola. *Stieltjes integral representation of effective diffusivities in time-dependent flows*. Phys. Rev. E, 52 (1995), 3249–3251.

[7] D. Bertacchi. *Asymptotic behaviour of the simple random walk on the 2-dimensional comb*. Electron. J. Probab, 11 (2006) 1184-1203.

[8] G. Boffetta, A. Celani, A. Crisanti, A. Vulpiani. *Pair dispersion in synthetic fully developed turbulence*. Phys. Rev. E, 60 (1999) 6734–6741.

[9] G. Boffetta, I. M. Sokolov. *Statistics of two-particle dispersion in two-dimensional turbulence*. Phys. Fluids 14 (2002), 3224–3232.

[10] B. Bollobás. Modern Graph theory. Springer-Verlag, New York, 1998.

[11] J.P. Bouchaud, A. Georges. *Anomalous diffusion in disordered media*. Phys. Rep., 195 (1990), 127–293.

[12] R. Burioni, D. Cassi. *Fractals without anomalous diffusion*. Phys. Rev. E, 49 (1994), R1785–R1787.

[13] R. Burioni, D. Cassi. *Spectral dimension of fractal trees*. Phys. Rev. E, 51 (1995), 2865–2869.

[14] R. Burioni, S. Chibbaro, D. Vergni, A. Vulpiani, *Reaction spreading on graphs*. Phys. Rev. E, 86 (2012), 055101–055104.

[15] D. Cassi, R. Sofia. *Random walks on d-dimensional comb Lattices*. Mod. Phys. Lett., B 6 (1992), 1397–1403.

[16] P. Castiglione, A. Mazzino, P. Muratore-Ginanneschi, A. Vulpiani. *On strong anomalous diffusion*. Physica D, 134 (1999), 75–93.

[17] J.W. Chamberlain, D.M. Hunten. Theory of Planetary Atmospheres: An Introduction to Their Physics and Chemistry. Academic Press, New York 1987.

[18] W.J. Cocke. *Turbulent Hydrodynamic Line Stretching: Consequences of Isotropy*. Phys. Fluids, 12 (1969), 2488–2492.

[19] M.E. Fisher. *Shape of a Self-Avoiding Walk or Polymer Chain*. J. Chem. Phys., 44 (1966), 616–622.

[20] R.A. Fisher. *The wave of advance of advantageous genes*. Ann. Hum. Genet., 7 (1937), 355–369.

[21] G. Forte, R. Burioni, F. Cecconi and A. Vulpiani, *Anomalous diffusion and response in branched systems: a simple analysis*. J. Phys.: Condens. Matter, 25 (2013), 465106.

[22] G. Forte, F. Cecconi and A. Vulpiani. *Non-anomalous diffusion is not always Gaussian*. Eur. Phys. J. B, 87 (2014), 102–111.

[23] M. Freidlin. Functional integration and partial differential equations. Princeton University Press, Princeton NJ, 1985.

[24] U. Frisch. Turbulence. The legacy of A.N. Kolmogorov. Cambridge University Press, Cambridge (UK) 1995.

[25] A. Gabrielli, F. Cecconi. *Diffusion, super-diffusion and coalescence from single step*. J. Stat. Mech. (2007), P10007.

[26] B. Gnedenko and A.N. Kolmogorov. Limit distribution for Sums of Independent Random Variables. Addison-Wesley, 1954.

[27] R. Ishizaki, T. Horita, T. Kobayashi, H. Mori. *Anomalous diffusion due to accelerator modes in the standard map*. Prog. Theor. Phys., 85 (1991), 1013–1022.

[28] J. Klafter and I.M. Sokolov. First steps in random walks: from tools to applications. Oxford University Press, New York, 2011.

[29] R. Klages. G. Radons. I.M. Sokolov. Anomalous transport: foundations and applications. Wiley-VCH Verlag GmbH & Co. Weinheim (DE) (2008).

[30] X.P. Kong and E.G.D. Cohen. *Anomalous diffusion in a lattice-gas wind-tree model*. Phys. Rev. B, 40 (1989), 4838-4845.

[31] J. Klafter, M. F. Shlesinger, G. Zumofen. *Beyond brownian motion*. Physics Today, 49 (1996), 33–39.

[32] A.N. Kolmogorov, I.G. Petrovskii, N.S. Piskunov, *A study of the diffusion equation with increase in the quantity of matter, and its application to a biological problem*. Bull. Moscow Univ. Math., A 1 (1937), 1–25.

[33] A.J. Lichtenberg, M.A. Lieberman. Regular and Chaotic Dynamics. Springer-Verlag, New York, 1991.

[34] A.J. Majda, P.R. Kramer. *Simplified models for turbulent diffusion: Theory, numerical modelling, and physical phenomena*. Phys. Rep., 314 (1999), 237–574.

[35] R. Mancinelli, D. Vergni and A. Vulpiani. *Superfast front propagation in reactive systems with anomalous diffusion*. Eur. Phys. Lett., (2002) 60, 532–538.

[36] R. Mancinelli, D. Vergni and A. Vulpiani. *Front propagation in reactive systems with anomalous diffusion*. Physica D, 85 (2003), 175–195.

[37] B. Mandelbrot. The Fractal Geometry of Nature. Freeman, San Francisco, 1983.

[38] T. Manos and M. Robnik. *Survey on the role of accelerator modes for anomalous diffusion: The case of the standard map*. Phys. Rev. E, 89 (2014), 022905.

[39] R.N. Mantegna, H.E. Stanley. *Stochastic process with ultraslow convergence to a Gaussian: The truncated Lévy flight*. Phys. Rev. Lett., 73 (1994), 2946–2949.

[40] G. Matheron, G. De Marsily. *Is transport in porous media always diffusive?*. Water Resources Res., 16 (1980), 901–917.

[41] V. Méndez, A. Iomin, D. Campos and W. Horsthemke. *M*esoscopic description of random walks on combs. Phys. Rev. E, 92 (2015), 062112.

[42] J.D. Murray. Mathematical Biology, Springer, Berlin 1993.

[43] Z. Neufeld and E. Hernández-García. Chemical and Biological Processes in Fluid Flows: A Dynamical Systems Approach. World Scientific, Singapore 2009.

[44] B. O'Shaughnessy, I. Procaccia. *Diffusion on fractals*. Phys. Rev. A, 32 (1985), 3073–3083;

[45] A. Okubo, S.A. Levin. Diffusion and Ecological Problems: Modern Perspectives, Science & Business Media vol. 14, Springer, Berlin 2013.

[46] H.R. Pruppacher, J.D. Klett. Microphysics of clouds and precipitation. Kluwer Academic Plubisher, Boston 1998.

[47] A.B. Rechester, R.B. White. *Calculation of turbulent diffusion for the Chirikov-Taylor model*. Phys. Rev. Lett., 44 (1980), 1586–1589.

[48] L.F. Richardson. *Atmospheric diffusion shown on a distance-neighbour graph*. Proc. R. Soc. Lond., A 110 (1926), 709–737.

[49] D.E. Rosner. Transport processes in chemically reacting flow systems. Butterworth-Heinemann, Boston 2013.

[50] M.F. Schlesinger, B. West, J. Klafter. *Lévy dynamics of enhanced diffusion: Application to turbulence*. Phys. Rev. Lett., 58 (1987), 1100–1104.

[51] N.G. Van Kampen. Stochastic processes in physics and chemistry. Elsevier, 1992.

[52] V.A. Volpert, Y. Nec, A.A. Nepomnyashchy, *Exact solutions in front propagation problems with superdiffusion*. Physica D, 239 (2010), 134–144.

[53] J.B. Weiss, A. Provenzale, eds. Transport and mixing in geophysical flows. vol. 744. Springer, Berlin 2007.

[54] G.M. Zaslavsky, D. Stevens, A. Weitzener. *Self-similar transport in incomplete chaos*. Phys. Rev. E, 48 (1993), 1683–1694.